*Phase Transitions*, 1995, Vol. 53, pp. 87–114
Reprints available directly from the publisher
Photocopying permitted by license only



# REVIEW

# STRUCTURAL PHASE TRANSITIONS AT CLEAN AND METAL-COVERED Si(111) SURFACES INVESTIGATED BY RHEED SPOT ANALYSIS

SHUJI HASEGAWA,*† YASUYOSHI NAGAI, TOSHIO OONISHI, NOBUHIKO KOBAYASHI, TAKASHI MIYAKE, SHUUICHI MURAKAMI, YUUJI ISHII, DAIKI HANAWA and SHOZO INO

*Department of Physics, Graduate School of Science, University of Tokyo, Hongo, Bunkyo-ku, Tokyo 113, JAPAN*
† *also PRESTO, Research Development Corporation of Japan (JRDC)*

*(Received 20 February 1994)*

Structural phase transitions between various kinds of superlattice structures formed on a Si(111) surface have been investigated by spot analysis of reflection high-energy electron diffraction (RHEED). Reversible transitions induced by temperature changes and irreversible ones induced by metal depositions were observed. Detailed discussions on the dynamics of the phase transitions are made by quantitative analyses of integrated spot intensity and profile. For a phase transition of $7\times7\leftrightarrow1\times1$ structures on a clean Si(111) surface, a hysteresis with temperature difference of 5°C between in heating and cooling processes was found in the spot intensity change, indicating a first-order transition. Hysteresis was hardly recognized, on the other hand, for transitions of Au-induced superstructures ($5\times2$-Au or $\sqrt{3}\times\sqrt{3}$-Au)$\leftrightarrow1\times1$-Au. The spot profiles were found to be broadened during the transition of Si(111)-$\sqrt{3}\times\sqrt{3}$-Au $\leftrightarrow1\times1$-Au, which was a signature of a continuous transition, while the profiles remained unchanged during the transitions of the $7\times7\leftrightarrow1\times1$ and $5\times2$-Au $\leftrightarrow1\times1$-Au phases. Structural conversions induced by In adsorption on the Si(111) surface kept at constant temperatures were also analyzed. The conversions at room temperature were totally dependent on the initial substrate surface structures; the $7\times7$ surface did not show any structural conversion with In adsorption, while the $\sqrt{3}\times\sqrt{3}$-In surface successively converted to a $2\times2$ and a $\sqrt{7}\times\sqrt{3}$ phase with coverage increase. The structural transitions at elevated temperatures were sensitively dependent on the temperatures. Sequences of transitions among the $7\times7$, $4\times1$, $\sqrt{3}\times\sqrt{3}$, $\sqrt{31}\times\sqrt{31}$, and $\sqrt{43}\times4$ were quantitatively revealed as changes in RHEED spot intensity.

KEY WORDS: Si(111) surface, RHEED, phase transition hysteresis

## 1 INTRODUCTION

In addition to static structures of atomic reconstructions and electronic states at solid surfaces, dynamic processes such as phase transitions of surface structures are also the

*Author for correspondence.

main subjects in surface science. This is partly because the reduced dimensionality of the system can induce a wider variety of phase transitions compared with three-dimensional (3D) bulk, and partly because surface restructurings are closely related to epitaxial growths of thin layers for device fabrication (for a review, see Bauer, 1987). Various kinds of sophisticated techniques have been employed for the study of phase transitions at surfaces (for example, Rivière, 1990). Changes in real space images can be directly obtained by various types of microscopy. Scanning tunneling microscopy (STM), in particular reveals detailed processes of structural changes on an atomic scale. This has clarified the important role of atomic structural irregularities, such as the role of step edges and defects in surface phase transitions. Diffraction methods, on the one hand, have still been powerful tools for characterizing phase transitions; the order (first or continuous transition), critical exponents, correlation lengths, and others can be deduced from diffraction experiments (for example, Nielsen, 1976). Phase transitions are thus fully understood with complementary information provided by both microscopy and diffraction methods.

We report here reflection-high-energy electron diffraction (RHEED) observations on structural phase transitions at clean and metal (Au or In) covered Si(111) surfaces, induced by temperature changes or metal-coverage changes. RHEED is now widely used as one of the most convenient tools for *in-situ* monitoring of the surface structures; (1) recognition of surface superstructures from the diffraction pattern, (2) precise monitoring of layer growths through intensity oscillations of the specular spot, and (3) detailed structural analysis by rocking curve measurements with dynamical scattering calculations. We present here another use of RHEED for analyzing dynamical changes of surface structures.

In Section 2, we deal with the phase transitions of a clean surface of Si(111), $7\times7 \leftrightarrow 1\times1$, and of Au-induced superlattice surfaces, Si(111)-$5\times2$-Au $\leftrightarrow$ $1\times1$-Au or Si(111)-$\sqrt{3}\times\sqrt{3}$-Au $\leftrightarrow$ $1 \times 1$-Au. These transitions are reversibly induced by heating or cooling across the critical temperatures. The intensities and profiles of the superlattice spots in RHEED are measured with precise temperature control to find temperature hysteresis and critical scattering during the transitions. In particular, we give detailed discussions on the transition at the clean Si(111) surface.

In Section 3, successive structural conversions on a Si(111) surface induced by continuous In deposition are observed as changes in intensities of superlattice spots. With increase of coverage at elevated temperatures, domains of superstructures successively convert from one to others; $7 \times 7 \rightarrow 4 \times 1$, $7 \times 7 \rightarrow \sqrt{3} \times \sqrt{3} \rightarrow \sqrt{31} \times \sqrt{31} \rightarrow 4 \times 1$, or $7 \times 7 \rightarrow \sqrt{3} \times \sqrt{3} \rightarrow \sqrt{43} \times 4 \rightarrow \sqrt{31} \times \sqrt{31}$, depending on the substrate temperature. By measuring the coverage at maximum intensity of the superlattice spot of each structure, its saturation coverage can be determined, assuming unity sticking coefficient of In atoms.

When In is deposited on a room-temperature Si(111)-$7 \times 7$ surface, any new superstructures do not appear; the $7\times7$ spots are only blurred. But the decrease in the spot intensity with In coverage is not monotonic; some superlattice spots temporarily became stronger before vanishing, while others only gradually fade out. This indicates some structural modification in the $7 \times 7$ unit cell during In adsorption. When In is deposited on a room-temperature pre-deposited Si(111)-$\sqrt{3} \times \sqrt{3}$-In surface, quite different phenomena are observed; surface structures successively change as $\sqrt{3} \times \sqrt{3} \rightarrow 2 \times 2 \rightarrow \sqrt{7} \times \sqrt{3} \rightarrow 1 \times 1$. The electrical resistance of the Si wafer, moreover, drastically drops synchronously with

these structural changes. In this case, structural phase transitions and In-layer growth styles crucially depend on the substrate surface structures.

## 2 PHASE TRANSITIONS INDUCED BY TEMPERATURE CHANGES

### *2.1 Background*

Following the first observation of a reversible transformation between $7 \times 7$ and $1 \times 1$ structures on a clean Si(111) surface around 850°C in low-energy electron diffraction (LEED) by Lander (1964), many groups have investigated the transition by a variety of experimental methods. But, from the literature, its generally accepted understanding seems very limited. Even the order of the phase transition is still controversial. In fact, in a recent monograph by Mönch (1993), this transition is reviewed and concluded to be a continuous phase transitien, although there are numerous other reports insisting on a first-order transition.

The nature of the transition inevitably depends on the structure of the $1 \times 1$-high temperature phase as well as the $7 \times 7$-dimer-adatom-stacking fault (DAS) structure (Takayanagi, Tanishiro, Takahash and Takahashi, 1985a, 1985b) at low temperature. RHEED observations (Ino, 1977, Chevrier, Vinh and Cruz, 1992) showed a gradual disappearance of the $7 \times 7$-superlattice spots without broadening at the transition during heating. Diffuse spots of a $\sqrt{3} \times \sqrt{3}$ (R30°) periodicity in the $1 \times 1$ phase were also found (Ino, 1977), which were observed also in LEED (Iwasaki, Hasegawa, Akizuki, Li, Nakanura and Kanamori, 1987). This indicates that the $1 \times 1$-high-temperature phase is not a simple truncated (111) face of a bulk crystal. From the striking observations of reflection electron microscopy (REM) (Osakabe, Tanishiro, Yagi and Honjo, 1981; Latyshev, Krasilnikov, Aseev, Sokolov and Stenin, 1991) and low-energy electron reflection microscopy (Telieps and Bauer, 1985), the transition was concluded to be of first order, because the $7 \times 7$- and $1 \times 1$-phase domains separately coexisted during the transition. But no appreciable hysteresis could be observed. Helium atom diffraction experiments (Ha and Greene, 1989) led to the conclusion of a first-order and order-disorder type transition. On the basis of rocking curve measurements in RHEED, Kohmoto and Ichimiya, (1989) also insisted on the same type of transitisn, but not a simple order-disorder process, and proposed a structural model of the $1 \times 1$ phase with adaton randomly adsorbed over a relaxed bulk-like surface. A similar model was discussed by Iwasaki *et al.* (1987). Adatoms on a $1 \times 1$ substrate were also concluded on by observing the shift of monatomic steps in REM images during the transition (Latyshev *et al.*, 1991). These adatoms are so highly mobile on the substrate that a high-temperature STM cannot image them (Kitamura, Sato and Iwatsuki, 1991). The first REM observation (Osakabe *et al.*, 1981) and also STM (Kitamura *et al.*, 1991) revealed that atomic step edges play an important role in the transition. The structural conversion always begins at step edges and spreads out on the terraces. Theoretical considerations from the point of view of symmetry change, furthermore, led to the conclusion that the $1 \times 1 \rightarrow 7 \times 7$ transition cannot proceed via a continuous phase transition (Blandin, 1973; Zangwill, 1988). A simulation based on a lattice gas model also suggested a first-order transition (Sakamoto and Kanamori, 1993).

On the contrary, in LEED observations (Florio and Robertson, 1970; Bennett and Webb, 1981), the continuous and gradual changes in spot intensities during the phase transition led to the conclusion of a second order transition and an order-disorder type, because of excess diffuse scattering appearing in place of the 7 × 7 spots. MacRae and Malic (1985) confirmed this conclusion from a detailed analysis of LEED spot profiles. Tanishiro *et al.* re-examined the contrast of the 7 × 7-domain in REM images (Tanishiro, Takayanagi and Yagi, 1983), and reversed the earlier conclusion (Osakabe *et al.*, 1981), suggesting a second-order transition.

In addition to such a controversy on the order of the phase transition, there is another interesting question as to whether a transient structure, that is different from the DAS model, exists or not during the phase transition. Some papers (Ishizaka, Doi and Ichikawa, 1991; Hricovini, LeLay, Abraham and Bonnet, 1990) suggest that a 7 × 7 unit cell consisting only of a dimer-stacking fault framework, with random adatom arrangement, can be temporarily created during the transition. These problems on this phase transition are closely related to homoepitaxy of Si on a Si(111) surface, in which the 7 × 7 structure on the substrate must reconstruct into a 1 × 1 to grow, and the surface of the Si epilayer reconstructs in turn into the 7 × 7 structure from a 1 × 1. This restructuring in Si homoepitaxy is discussed in detail by Tochihara, Shimada, Itoh, Tanaka, Udagawa and Sumita (1992).

### 2.2 *Experimental*

We again measured the intensity changes of the 7 × 7 superlattice spots in RHEED during the phase transition with precise temperature control. A hysteresis with a temperature difference of about 5°C was observed in the intensity changes between heating and cooling across the transition temperature (Hasegawa, Nagai, Oonishi and Ino, 1993). The phase transition then settled down to be of first order. During the transition, moreover, the intensity ratios among the 7 × 7 superlattice spots did not show appreciable changes. This indicates that the DAS structure in the 7 × 7 unit cell remains during the structural transition, and directly converts into the 1 × 1 structure without passing through any transient phase. For comparison, similar measurements for reversible structural transitions at Au deposited Si(111) surfaces were carried out. In transitions between Au-induced superstructures, Si(111)-5 × 2- or -$\sqrt{3} \times \sqrt{3}$-Au (Ino, 1988) ↔ 1 × 1-Au phases, appreciable hysteresis could not be observed within our experimental precision. The spot profile was found to be broadened in the $\sqrt{3} \times \sqrt{3}$-Au ↔ 1 × 1-Au transition, while the profiles did not significantly change at the transitions of the clean 7 × 7 ↔ 1 × 1 and the 5 × 2-Au ↔ 1 × 1-Au. So only the $\sqrt{3} \times \sqrt{3}$-Au ↔ 1 × 1-Au transition was concluded to be continuous.

The experiments were performed with a conventional ultra-high vacuum chamber with a RHEED system of 15 kV acceleration (Ino, 1977) and metal-evaporation sources of alumina-coated W baskets. A *p*-type Si(111) wafer of 8–18 mΩ cm resistivity and 25 × 4 × 0.4 $mm^3$ size was used. The surface was cleaned by several flash heatings up to 1200°C with a DC current of 9.0 A fed through the wafer, followed by cooling. On cooling, a temporary annealing for about 30 sec or more at a temperature just below the 1 × 1 → 7 × 7 transition (700~750°C) was carried out to make the structural conversion undergo completely on the whole surface (Bennett and Webb, 1981; Tanishiro *et al.*, 1983; Phaneuf, Bartelt,

Williams, Świech and Bauer, 1992), resulting in a clear 7 × 7-RHEED pattern at room temperature (RT).

The sample temperature was controlled by DC heating current supplied by a stabilized power supply (ADVANTEST model TR6162) in constant current mode. The temperature was measured with an optical pyrometer, with an estimated accuracy of ±20°C. Since the temperature (T) is empirically related to the heating current (I) through $\log T \propto \log I$ (Ichikawa and Ino, 1981), a calibration curve could be made to convert the current reading into temperature. The precise control of relative change in temperature was then easily achieved with good reproducibility by accurate control of the digital-set heating current and sufficient waiting time for sample temperature stabilization, although absolute values of temperature were not accurately determined in the present study. In fact the critical temperature of the 7 × 7 ↔ 1 × 1 transition in this report (800°C) seems slightly lower than the values (830–870°C) in the literatures. A temperature change of 1°C corresponded to a current change of about 10 mA at the transition around 800°C with a heating current of 2 A. Starting from 760°C in the 7 × 7 phase (after maintained for about 10 min at this temperature for stabilization), we heated the sample stepwise with about 1°C increments up to 805°C to convert the surface into the 1 × 1 phase. 30 sec or 1 min was allowed at each temperature step to let the system equilibrate. At each temperature, a picture of the RHEED pattern was successively taken with a TV camera (HAMAMATSU model C2741) in 512 × 480 × 8bit format through 32 frames averaged, and stored on a magneto-optical disk. Symmetrically the same measurements were followed on cooling, starting from 805°C in the 1 × 1 phase down to 760°C to return to the 7 × 7 one. After successive measurements both on heating and cooling across the transition, which took 45 min or 90 min in total, the integrated intensities and profiles of individual superlattice spots were analyzed from the stored image data with an image processing computer (NIRECO model LUZEX IIIU).

### *2.3 Results and discussions*

The RHEED patterns taken successively during this phase transition are shown in Fig. 1. Figure 2 shows the measured temperature dependence of the integrated spot intensity of the $(\frac{1}{7}, \frac{3}{7})$ superlattice reflection during the transition (without correction for the Debye-Waller (DW) factor). Hysteretic changes with temperature difference of about 5°C are noticed during steep changes in intensity in the interval of 785–800°C heating and cooling, while the relatively slow temperature dependence over the region below 785°C coincides with each other. The same hysteretic changes were also observed with other non-equivalent 7 × 7-superlattice reflections. The results are independent of the waiting time of each temperature step on heating/cooling 30 sec or 1 min. We also carried out two successive series of heating/cooling processes, i.e. heating→cooling→heating→cooling across the transition temperature to confirm the reproducibility. From the reason mentioned below, the sample temperature was believed to be equilibrated to within at least 1°C precision at each temperature step both on heating and cooling. At each temperature increment of negative or positive over the temperature range presented, the voltage drop between a pair of voltage pick-up contacts of a 4-probe-resistance-measurement sample holder (Hasegawa and Ino, 1992) during the flow of heating current, swiftly stabilized to within $\frac{1}{1000}$ of its value within a few seconds. The voltage drop divided by the current follows the temperature dependence

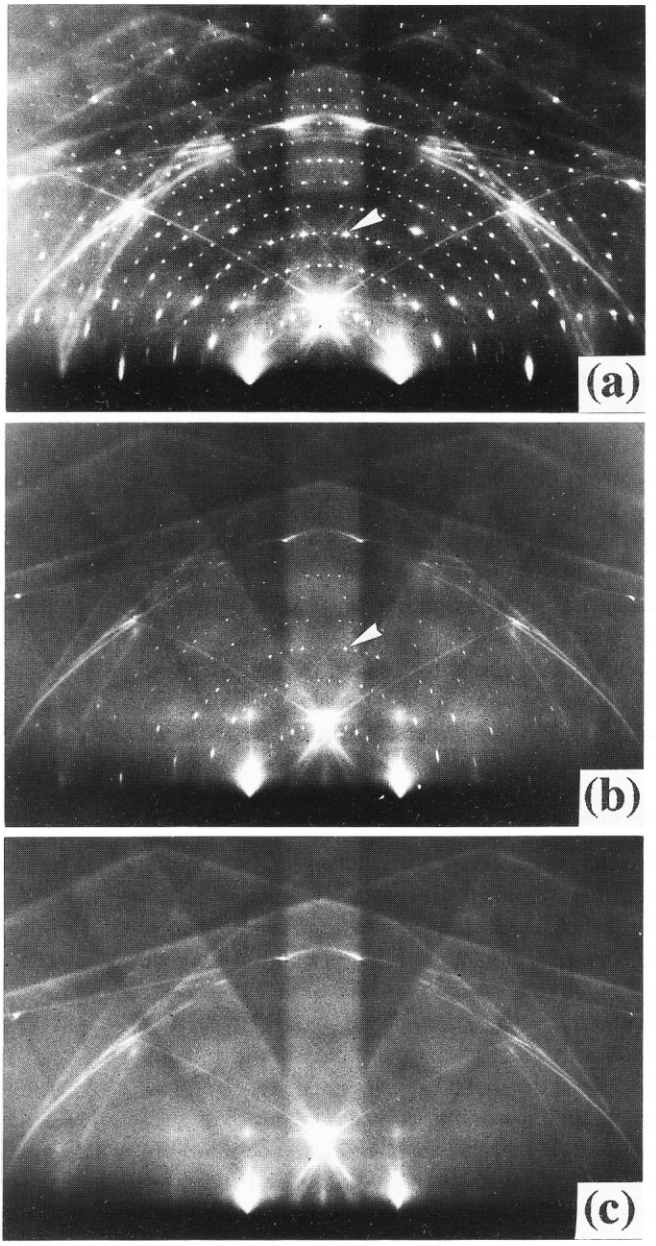


**Figure 1** The RHEED patterns taken from a clean Si(111)-7×7 surface (a) at room temperature, (b) just below and (d) just above the critical temperature of the phase transition of $7\times7\leftrightarrow1\times1$. The electron beam was accelerated up to 15 kV in [11$\bar{2}$] incidence.

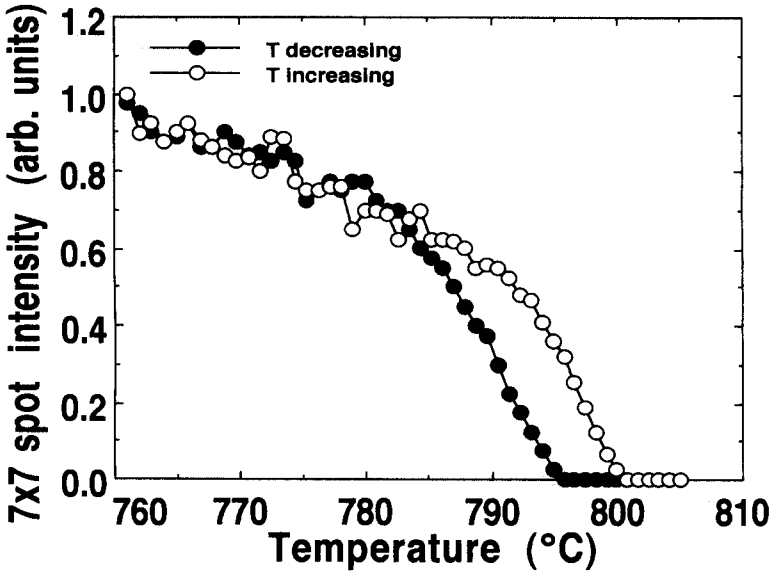


**Figure 2** The temperature dependence of the integrated intensity of the $(\frac{1}{7}, \frac{3}{7})$-th superlattice spot in the Si(111)-7×7 RHEED pattern during heating and cooling processes across the transition temperature.

$\exp(-E_g/2kT)$ at elevated temperatures, where $E_g$ is the band-gap energy for Si. This is the same as that for the resistance of an intrinsic semiconductor, which is very sensitive to temperature. Therefore, the temperature stabilization may be confirmed with this voltage drop.

Although a similar temperature difference of about 3°C between the warming and cooling curves across the transition was reported in a LEED experiment by Bennett and Webb (1981), they did not prove the existence of hysteresis, rather attributing that the intensity on the cooling curve had not reached a steady value because of slow equilibration rate. According to them, the $7 \times 7$-superlattice spot intensity slowly equilibrates with a $t^{-1/2}$-diffusive tail after an initial period of exponential relaxation in the case of the $1 \times 1 \rightarrow 7 \times 7$ transition by negative temperature increment ($t$ is time). We carried out similar experiments as theirs, in which the temperature was suddenly dropped across the transition and the time evolution of the superlattice-spot intensity was monitored. Figure 3 shows the results which confirm that the spot intensity reaches its equilibration value at most within 20 sec, fairly shorter than their results. So we can safely say that, in our observations, the spot intensity as well as the temperatures were equilibrated at each temperature step with 30-sec intervals. The hysteretic change confirmed in this way is now an unequivocal signature of a first-order transition. As discussed later, some reasons such as strain field (Chevrier *et al.*, 1992; Zangwill, 1988; Tanishiro *et al.*, 1983) may increase the apparent broadening of the transition.

We also measured changes in intensity ratio of each superlattice spot to that of the $(\frac{2}{7}, \frac{2}{7})$ spot during the transition. The fractional order spots of $(\frac{3}{7}, 0)$, $(\frac{4}{7}, 0)$, $(\frac{3}{7}, \frac{1}{7})$, $(\frac{4}{7}, -\frac{1}{7})$ and

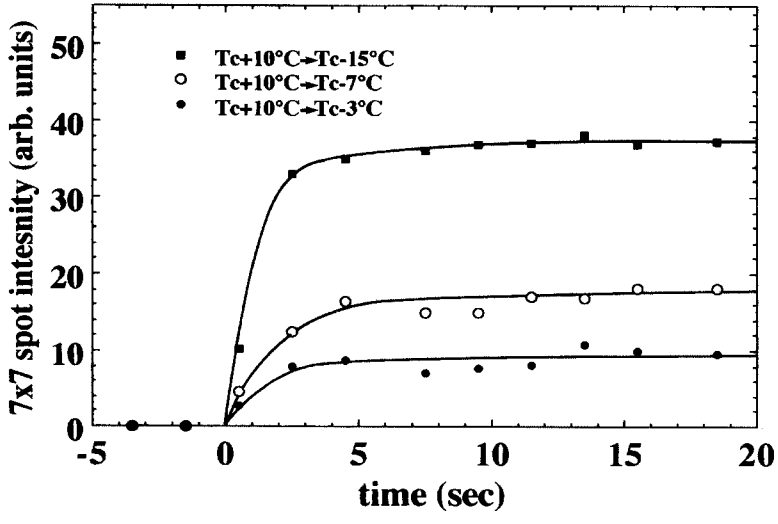


**Figure 3** The growth of the 7×7 superlattice spot intensity caused by sudden temperature decrease from a temperature above the transition ($T_c$) down to a temperature below it. The initial high temperature was fixed to be 10°C above the $T_c$, and the final temperatures were varied, 15°C, 7°C, and 3°C below the $T_c$. The images of the RHEED pattern were taken into an image processing computer with time intervals of 3 sec.

equivalent ones in the 7 × 7-RHEED pattern from the clean Si(111) surface are known to be stronger than other superlattice reflections, due to interference of waves scattered from adatom-arrays of a 2 × 2 periodicity in the DAS unit (Ino, 1980a, 1980b). As shown in Fig. 4(b), the intensity ratios remain almost constant, though the experimental error just before the disappearance of the spots is fairly large. This means the 2 × 2-adatom arrangement in the 7 × 7-unit cell is conserved until the 7 × 7 structure is completely destroyed into the 1 × 1 phase. In other words, this structural conversion is not triggered by randomizing the adatom arrangement in the 7 × 7 unit cell, but rather the dimer-stacking fault framework is dissolved at the same time with the topmost adatom layer. Reversibly, the conversion of 1 × 1 → 7 × 7 also seems to proceed by simultaneous construction of each 'constituent' in the DAS unit. In conclusion, there seems no transient structure such as a '$\delta - 7 \times 7$' structure (Daimon and Ino, 1985; Horio, Ichimiya, Kohmoto and Nakahara, 1991) during the transition, which seems consistent with STM observation (Kitamura *et al.*, 1991), while some reports suggest a transient structure of a 7 × 7 periodicity without ordered adatoms near the transition (Ishizaka, *et al.*, 1991; Hricovini *et al.*, 1990).

As observed by REM (Osakabe *et al.*, 1981, Latyshev *et al.*, 1991, Tanishiro *et al.*, 1983) and STM (Kitamura *et al.*, 1991), the atomic step configuration on the surface varies and 2D sublimation islands appear on the terrace due to redistribution of Si atoms during the $7 \times 7 \leftrightarrow 1 \times 1$ transition. Such a displacive transition is considered to be strongly influenced by impurities, defects, and strains on the surface. Bauer (1987) suggests that in the carbon-contamined region the transition temperature is reduced because of the 1 × 1-stabilizing and step-pinning effects by the carbon. This is the reason why the apparent continuous

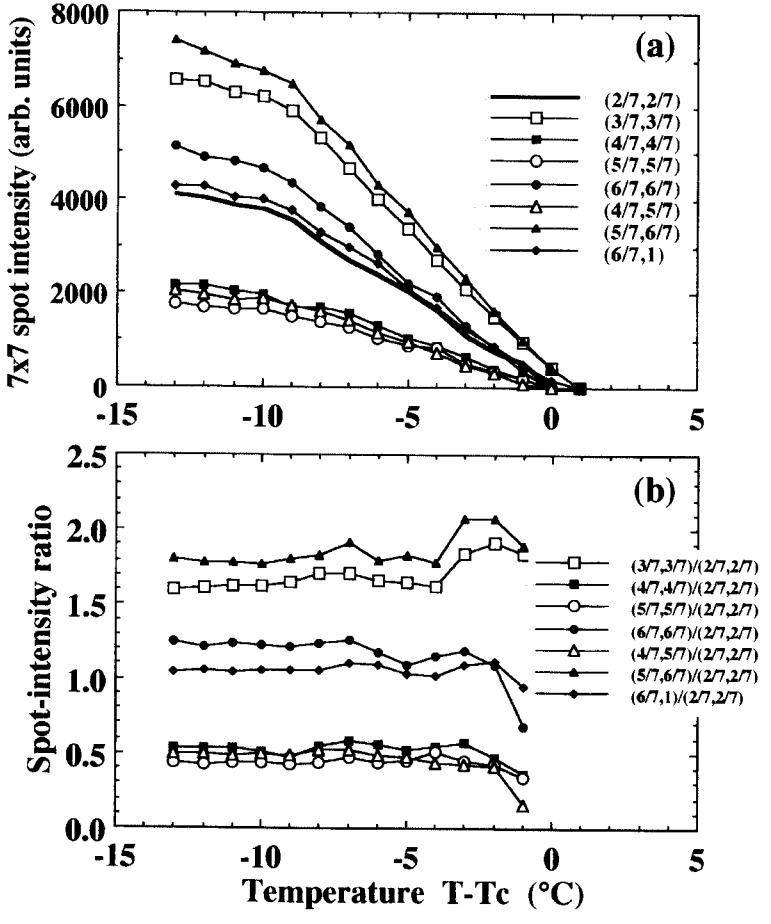


**Figure 4** The temperature dependence of (a) the integrated intensities of the superlattice spots and (b) their ratios to the intensity of the $(\frac{2}{7}, \frac{2}{7})$-th spot in the 7×7 RHEED pattern during the phase transition.

transition occurred over a wide temperature range of about 50°C in the previous diffraction experiments (Florio and Robertson, 1970, Bennet and Webb, 1981), while the transition temperature range observed in the microscopy studies (Osakabe *et al.*, 1981, Telieps and Bauer, 1985) is only around 10°C. Looking at the steep decrease of the 7 × 7 spot intensity in the range of 785–795°C in the cooling process and 790–800°C in the warming process in Fig. 2, the transition in our experirment seems to take place in a temperature range as narrow as the previous microscopy observations (compare Fig. 2 in the present study with Fig. 5 in the paper by Osakabe *et al.* (1981)). From this consideration, we believe that trace carbon negligibly affects our results.

In addition to carbon contamination, a high density of irregular steps and other kinds of defects will seed the phase transition because of strain fields on the surface. These make it

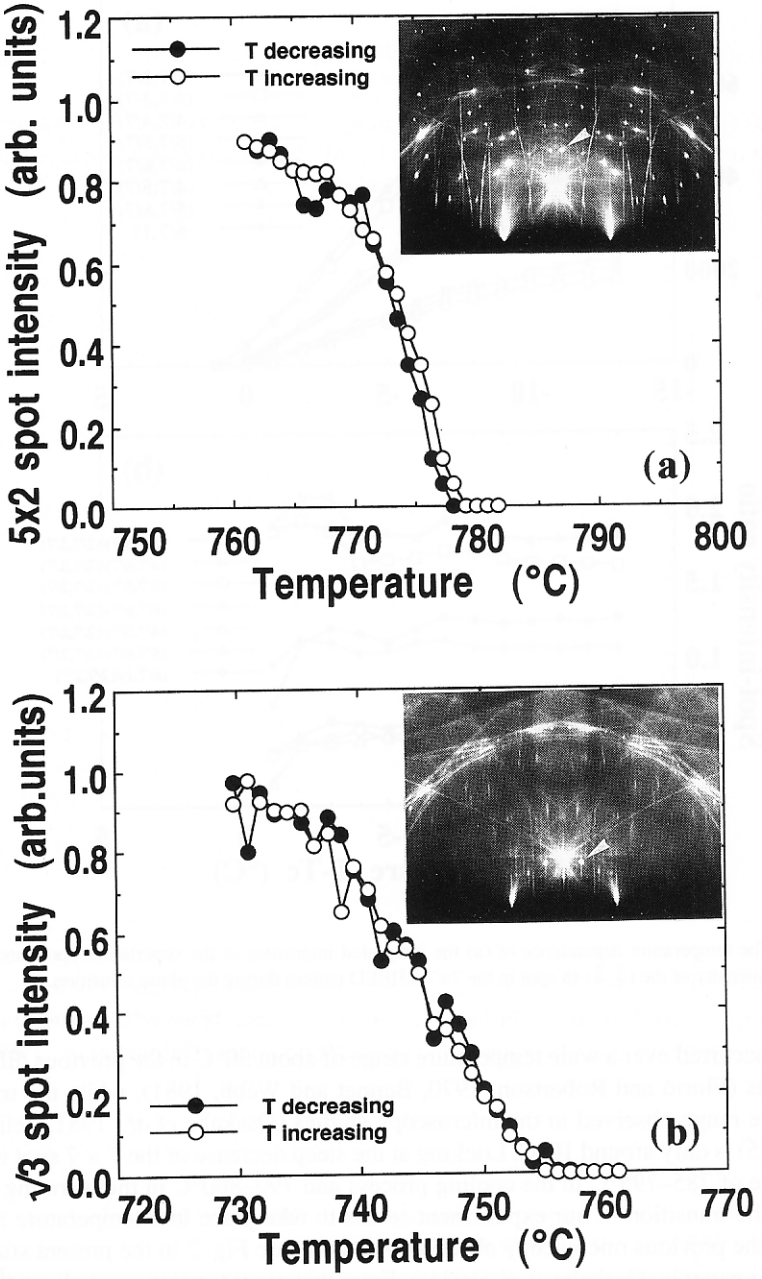


**Figure 5** The temperature dependence of the integrated intensity of the superlattice spots in the RHEED patterns of (a) Si(111)-5×2-Au (inserted pattern), and (b) Si(111)-$\beta-\sqrt{3}\times\sqrt{3}$-Au (inserted pattern), respectively, during heating and cooling across the respective transition temperatures.

difficult to observe hysteresis with a metastable surface in the truly thermodynamical sense of an ideal system. So there is a possibility that the hysteretic change reported here depends upon the densities of steps and/or defects such as domain boundaries on the surface. Similar measurements, then, may be needed with step-bunched or -anti-bunched surfaces, or vicinal surfaces.

Figure 5(a) shows similar changes in the integrated intensity of the $(0, \frac{1}{5})$ superlattice reflection from the $5 \times 2$ structure with about 0.5 ML(monolayer) Au coverage (Ino, 1988; Daimon, Chung, Ino and Watanabe, 1990; Tanishiro, Yagi and Takayanagi, 1990; Baski, Nogami and Quate, 1990; Bauer, 1991) without correction for the DW factor. In contrast to Fig. 2, we cannot conclude the existence of hysteresis with good reason although a temperature difference of about 1°C between the heating and cooling curves is seen. In the $\beta - \sqrt{3} \times \sqrt{3}$-Au (about 1 ML Au coverage) $\leftrightarrow 1 \times 1$-Au transition (Ino, 1988; Nogami, Baski and Quate, 1990), as shown in Fig. 5(b), the intensity of the $(\frac{1}{3}, \frac{1}{3})$ superlattice spot gradually changes in a wider temperature range compared with the curves in Figs. 2 and 5(a). Any hysteresis is again hardly recognized. In this way, negligible hysteresis at these transitions on Au-induced-superstructure surfaces may ensure our experimental precision of temperature control.

In addition to the temperature dependence of the integrated intensity of the superlattice spots mentioned above, the changes in the spot profile were also analyzed from the stored image data. Figure 6 shows the profiles along the vertical line in the $[1\bar{1}2]$-incidence RHEED patterns for (a) the $7 \times 7$, (b) $5 \times 2$-Au, and (c) $\beta - \sqrt{3} \times \sqrt{3}$-Au superlattice spots, respectively, during their disappearances on heating. In the former two surfaces (a) and (b), the spots seem to decrease their intensity without appreciable profile changes, while the $\beta - \sqrt{3} \times \sqrt{3}$-Au spot becomes broader and streaky on approaching the transition. The streak remains after disappearance of the sharp peak in (c). This is similar to LEED observations of the phase transition undergone on a clean Si(100) surface at about 200K between a $c(4 \times 2)$ at lower temperature and a $2 \times 1$ at higher temperature (Murata, Kubota and Tabata, 1992; Tabata, Aruga and Murata, 1987). So the phase transition of Si(111)-$\beta$-$\sqrt{3} \times \sqrt{3}$-Au $\leftrightarrow 1 \times 1$-Au is concluded to be continuous. Detailed analysis to obtain the critical exponents are now in progress.

Although we cannot conclude at present whether the transitions of $5 \times 2$-Au $\leftrightarrow 1 \times 1$-Au are of first order or continuous (Świech, Bauer and Mundschau (1991) concluded this transition to be first-order), negligible hysteresis during this transition is distinctly different from the appreciable hysteresis for the $7 \times 7 \leftrightarrow 1 \times 1$ case. If we adopt structural models for Au-induced superstructures such as the open inferred ones (Daimon *et al.*, 1990; Bauer, 1991) in that Au atoms are arranged over a bulk-like Si(111) substrate, the negligible hysteresis is attributable to order-disorder processes involving only the Au adsorbates (1 ML or less) without rearrangement of Si atoms in the substrate, while the appreciable hysteresis for the $7 \times 7 \leftrightarrow 1 \times 1$ case originates from rearrangement of Si atoms in at least the DAS layer (2ML or more) which needs much more latent heat. In this sense, the $7 \times 7 \leftrightarrow 1 \rightarrow 1$ transition could be said to be more 3D-bulk like.

For comparison, we observed a melting-crystallization transition of 3D crystals, which is known to be a first-order transition with latent heat of melting. Al of about 20 ML deposited onto a Si(111)-$7 \times 7$ surface at RT grows epitaxially in that $(111)_{Si}//(001)_{Al}$, $\langle 11\bar{2}\rangle_{Si}//\langle 010\rangle_{Al}$ (Fig. 7(a)). On heating this Si wafer, the Al layer melted at around 684°C,

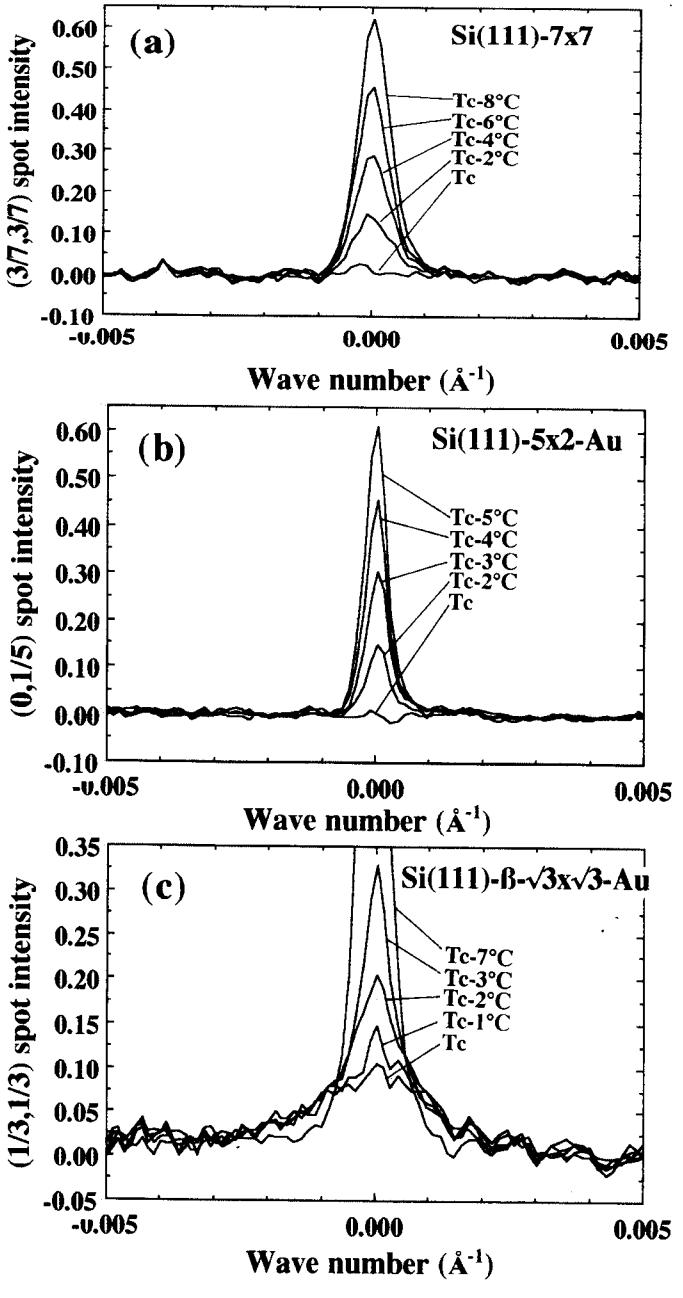


**Figure 6** The temperature dependence of the profiles of the superlattice spots from (a) the clean Si(111)-7×7, (b) Si(111)-5×2-Au, and (c) -$\beta-\sqrt{3}-\sqrt{3}$-Au surface, respectively, just below the respective transition temperatures ($T_c$). The profiles were along the vertical lines in the [11$\bar{2}$]-incidence RHEED patterns.

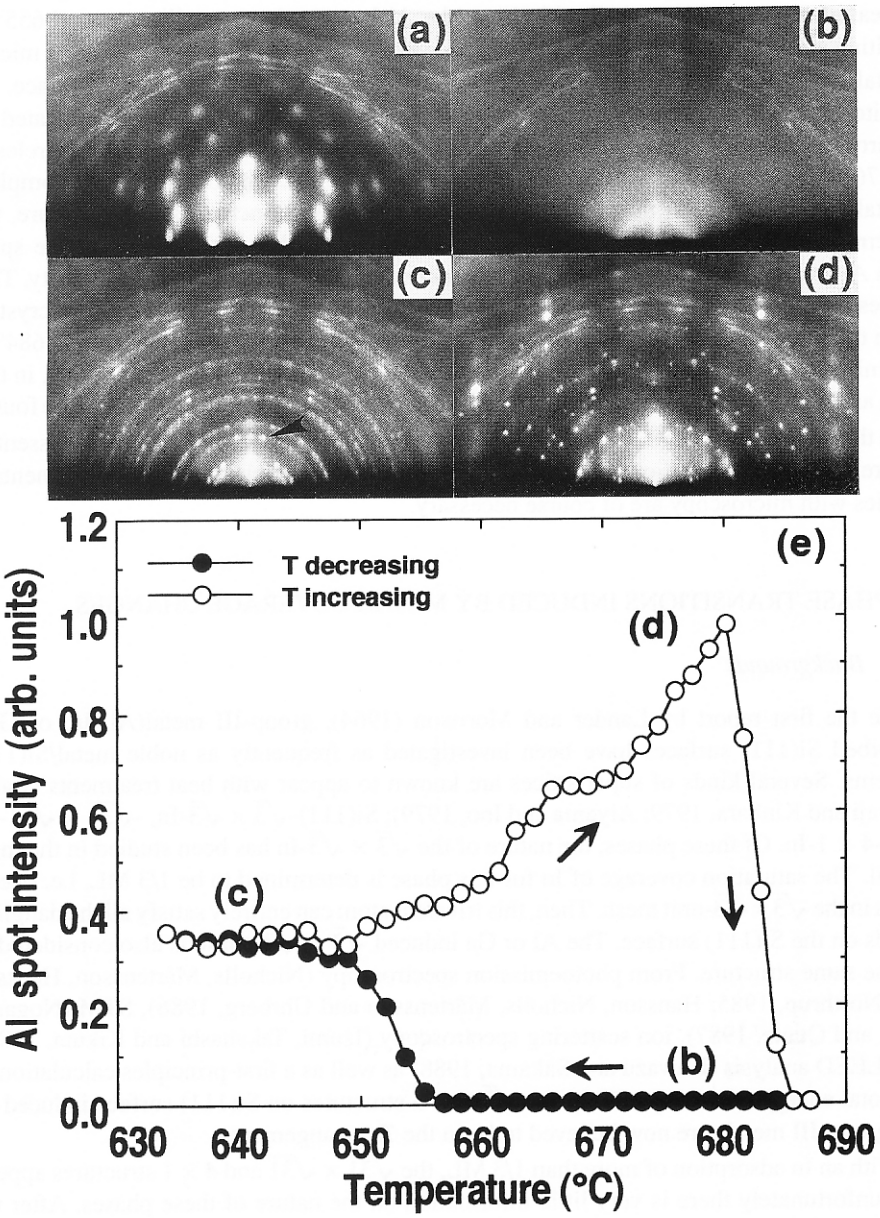


**Figure 7** RHEED patterns from a surface (a) after the room-temperature deposition of 20ML Al onto a clean Si(111)-7×7, (b) after melting of the Al layer by heating, (c) after its re-crystallization by cooling, and (d) after rearrangement of the microcrystals caused by heating up to just below the melting temperature, respectively. The variations in the patterns (b)→(c)→(d)→(b) were repeated in the cooling-heating cycles. (e) Peak intensities of the (220) diffraction spot from Al crystals, indicated by an arrow head in (c), as a function of temperature. The temperatures, at which the patterns (b)–(d) are observed, are indicated on the curve.

showing a halo pattern in RHEED (Fig. 7(b)). Next, when the temperature gradually decreased stepwise from this liquid phase, the Al began to re-crystallize around 655°C, resulting in a kind of Debye-ring pattern of Fig. 7(c). This indicates the growth of Al micro-crystals in random orientations including slight preferential orientations on the surface. By monitoring the peak intensity at the position of the 220 diffraction spot for Al (indicated by the arrow head in Fig. 7(c)), this solidification process is traced as a curve of solid circles in Fig. 7(e). The spot almost suddenly appeared at 655°C with crystallization. After complete crystallization at 635°C, the sample was heated again. With increase of temperature, the pattern changed from Fig. 7(c) to (d) before melting, in that the intensity of the spots from Al crystals in preferential orientations increased at the cost of the ring intensity. This process is shown as a curve of open circles in Fig. 7(e). This implies that Al micro-crystals align themselves along particular orientations. Finally, the crystals melted again at 684°C, returning to the pattern of Fig. 7(b). In the structural transition of Al micro-crystals, in this way, asymmetrical behavior as well as a temperature hysteresis as large as 30°C were found.

In this way, comparative studies such as the present one using RHEED reveal the essential nature of the phase transitions of surface structures and fine particles, though complementary studies with microscopy are of course necessary.

## 3 PHASE TRANSITIONS INDUCED BY METAL-COVERAGE CHANGES

### *3.1 Backgrounds*

Since the first report by Lander and Morrison (1964), group-III metal(Al, In, or Ga)-adsorbed Si(111) surfaces have been investigated as frequently as noble metal/Si(111) systems. Several kinds of superlattices are known to appear with heat treatments (Baba, Kawaji and Kinbara, 1979; Aiyama and Ino, 1979); Si(111)-$\sqrt{3} \times \sqrt{3}$-In, -$\sqrt{31} \times \sqrt{31}$-In, and -4 × 1-In. Of these phases, the nature of the $\sqrt{3} \times \sqrt{3}$-In has been studied in the most detail. The saturation coverage of In for this phase is determined to be 1/3 ML, i.e. one In atom in the $\sqrt{3} \times \sqrt{3}$-unit mesh. Then, this trivalent atom can entirely satisfy all the dangling bonds on the Si(111) surface. The Al or Ga induced $\sqrt{3} \times \sqrt{3}$ phase is also considered to be the same structure. From photoemission spectroscopy (Nicholls, Mårtensson, Hansson and Northrup, 1985; Hansson, Nicholls, Mårtensson and Uhrberg, 1986), STM (Nogami, Park and Quate, 1987), ion scattering spectroscopy (Izumi, Takahashi and Kikuta, 1989), and LEED analysis (Kawazu and Sakama, 1988) as well as a first-principles calculation of the total energy (Northrup, 1984), the $\sqrt{3} \times \sqrt{3}$ structures on Si(111) surface induced by the group-III metals are now believed to be in the $T_4$ arrangement.

With an In adsorption of more than 1/3 ML, the $\sqrt{31} \times \sqrt{31}$ and 4 × 1 structures appear. But unfortunately there is very little information on the nature of these phases. After the completion of the 4 × 1 structure, epitaxial growth of ordered In islands is observed at still higher coverages by annealing (Nogami *et al.*, 1987). Since the dangling bonds are totally saturated in the 4 × 1 phase, the In adatoms on top of this phase easily move as revealed in electromigration studies (Yasunaga, Kubo and Okuyama, 1986).

In this section, RHEED spot analysis is applied to observe the phase transitions induced by In adsorption onto a Si(111) surface kept at constant temperatures.

### 3.2 *In adsorption on Si(111)-7 × 7 at room temperature*

At first, In adsorption onto a clean Si(111)-7 × 7 surface at room temperature was analyzed. Figure 8 shows a series of RHEED patterns with continuous In deposition. Around 0.3 ML coverage of In (Fig. 8(b)), the relative intensities among the 7 × 7 superlattice reflections change from those of the clean 7 × 7 surface (Fig. 8(a)); for example, similar intensities of the superlattice spots on the 0th Laue zone in (b) should be compared with those in (a) where the $\frac{3}{7}$-th and $\frac{4}{7}$-th spots are especially strong. With further adsorption of In, the 7 × 7 super-reflections gradually blur (Figs. 8(c)(d)(e)), and finally disappear around 3 or 4 ML coverage. This process is revealed in more detail as changes in integrated intensities of the 7 × 7 superlattice spots as a function of In deposition time (Fig. 9). The blurring processes are not simple. Some superlattice spots temporarily increase their intensities during In deposition, while other spots monotonically fade out. The temporal intensity maxima of the spots occur at two different coverages; about 1/6 ML (95-sec deposition time, indicated by "A") and 1/3 ML (145 sec, indicated by "B"). The change of the relative intensities among the superlattice spots means some structural modifications in the 7 × 7-unit cell. Figure 10 shows the roughly estimated intensity of each superlattice spot in the $[11\bar{2}]$-incidence RHEED pattern from (a) a clean 7 × 7, and (b) and (c) with In adsorption of coverages indicated by "A" and "B", respectively, in Fig. 9. For the clean 7 × 7 surface, the $(\frac{3}{7}, \frac{3}{7})$-th and $(\frac{4}{7}, \frac{4}{7})$-th reflections show extra intensities which originate from the adatom array in a 2 × 2 periodicity in the DAS structure. This feature is reproduced by a kinematical calculation with atomic coordinates determined by Horio and Ichimiya (1989) based on the DAS structure, as shown in Fig. 10(d). This intensity distribution totally changes by In adsorption of sub-monolayer coverage. The distribution of Fig. 10(c), in which the $(\frac{3}{7}, \frac{4}{7})$ spot is especially strong and the $(\frac{3}{7}, \frac{1}{7})$ spot is weakened, is well simulated by a similar kinematical calculation as shown in Fig. 10(e) if adatoms are neglected from the 7 × 7-DAS structure. Then it is concluded that In adsorption of coverage corresponding to Fig. 10(c) makes the 2 × 2-adatom array in the DAS unit cell at random, remaining a 7 × 7 periodicity with only the dimer-stacking fault framework. The transient structure corresponding to the intensity distribution of Fig. 10(b) with smaller In coverage is not yet clarified.

### 3.3 *In adsorption on Si(111)-$\sqrt{3} \times \sqrt{3}$-In at room temperature*

Quite different phenomena are observed during the In adsorption onto a pre-deposited substrate, Si(111)-$\sqrt{3} \times \sqrt{3}$-In surface, at room temperature. A series of RHEED patterns is shown in Fig. 11. Starting from the $\sqrt{3} \times \sqrt{3}$ structure (Fig. 11(a)), 2 × 2 (b) and $\sqrt{7} \times \sqrt{3}$ (c) phases successively appear completed around 1 and 2 ML, respectively. With further deposition of In, superlattice spots disappear and only the fundamental spots with streaks from epitaxial In flat islands are observed in (d). In the $\sqrt{7} \times \sqrt{3}$ RHEED pattern (c), some superlattice points are observed in a limited range of the electron-beam glancing angle, meaning that this phase is composed of several In atomic layers (Tsuno, 1990).

The sequence of structural conversions is revealed as intensity changes of the respective superlattice spots (Fig. 12). In place of the $\sqrt{3} \times \sqrt{3}$ spot, the 2 × 2 spot becomes stronger almost linearly with In coverage increase. After passing its maximum intensity, it linearly goes to zero, and in turn, the $\sqrt{7} \times \sqrt{3}$ spot begins to grow. The saturation coverage of the

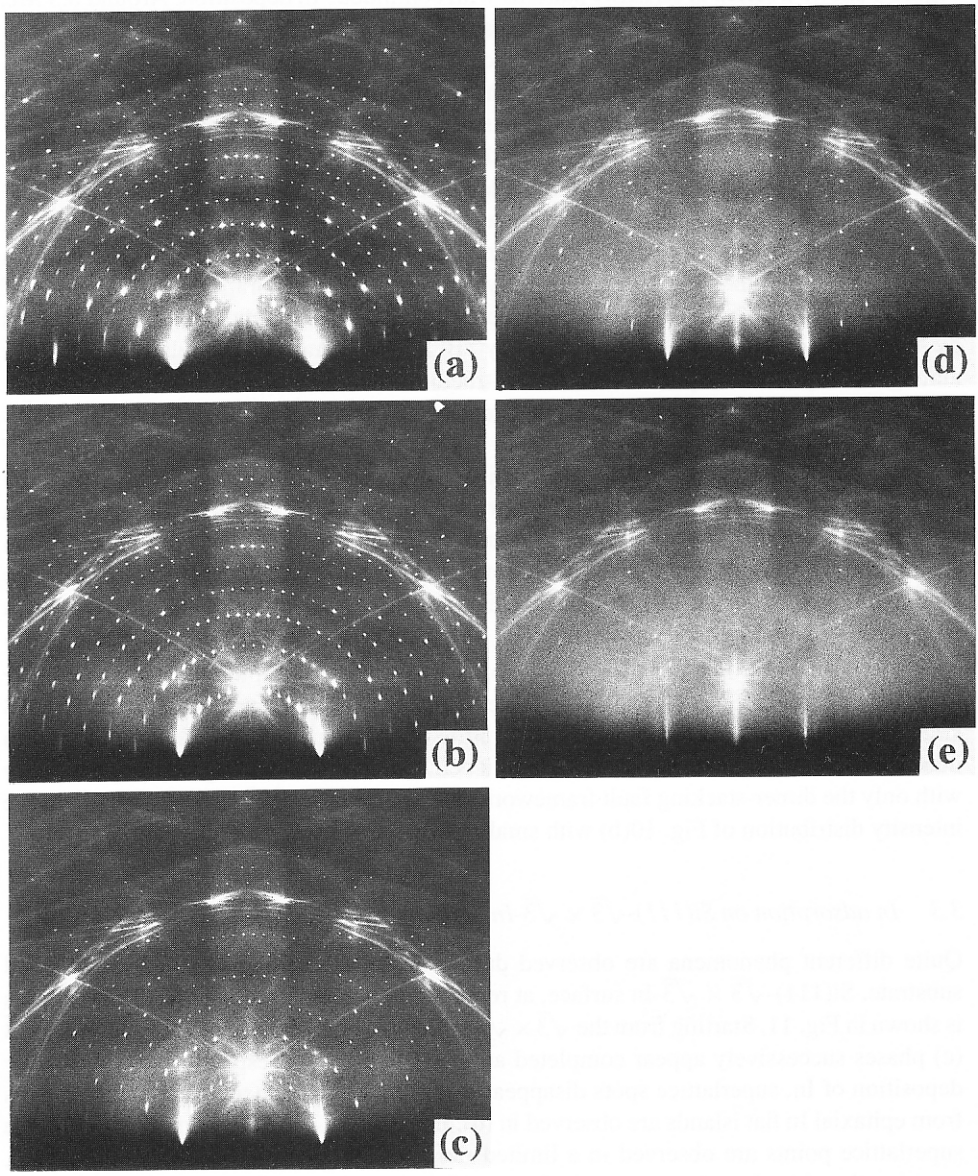


**Figure 8** A series of RHEED patterns during In deposition onto a clean Si(111)-7×7 surface at room temperature. In the 7×7 superlattice spots blurring out, the relative-intensity ratios among them changes with coverage increase.

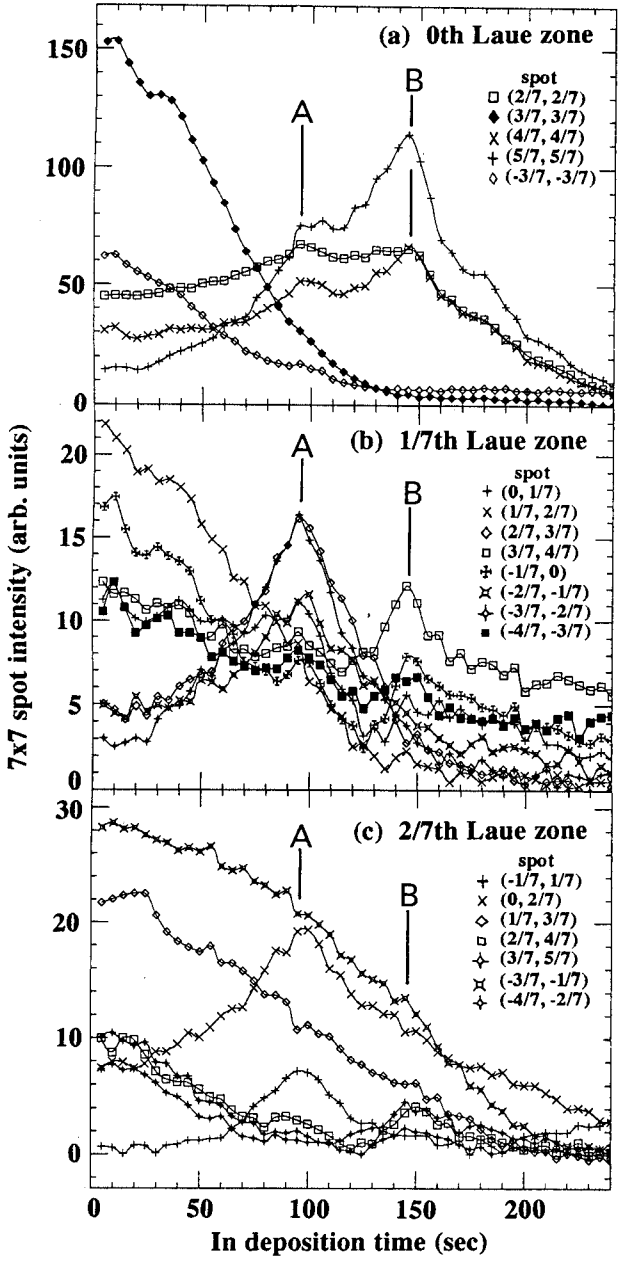


**Figure 9** The changes in the integrated intensities of the superlattice spots on the (a) 0-th, (b) $\frac{1}{7}$-th, and (c) $\frac{2}{7}$-th Laue zones, respectively, in the [11$\bar{2}$]-incidence RHEED patterns during In deposition onto the clean Si(111)-7×7 surface at room temperature.

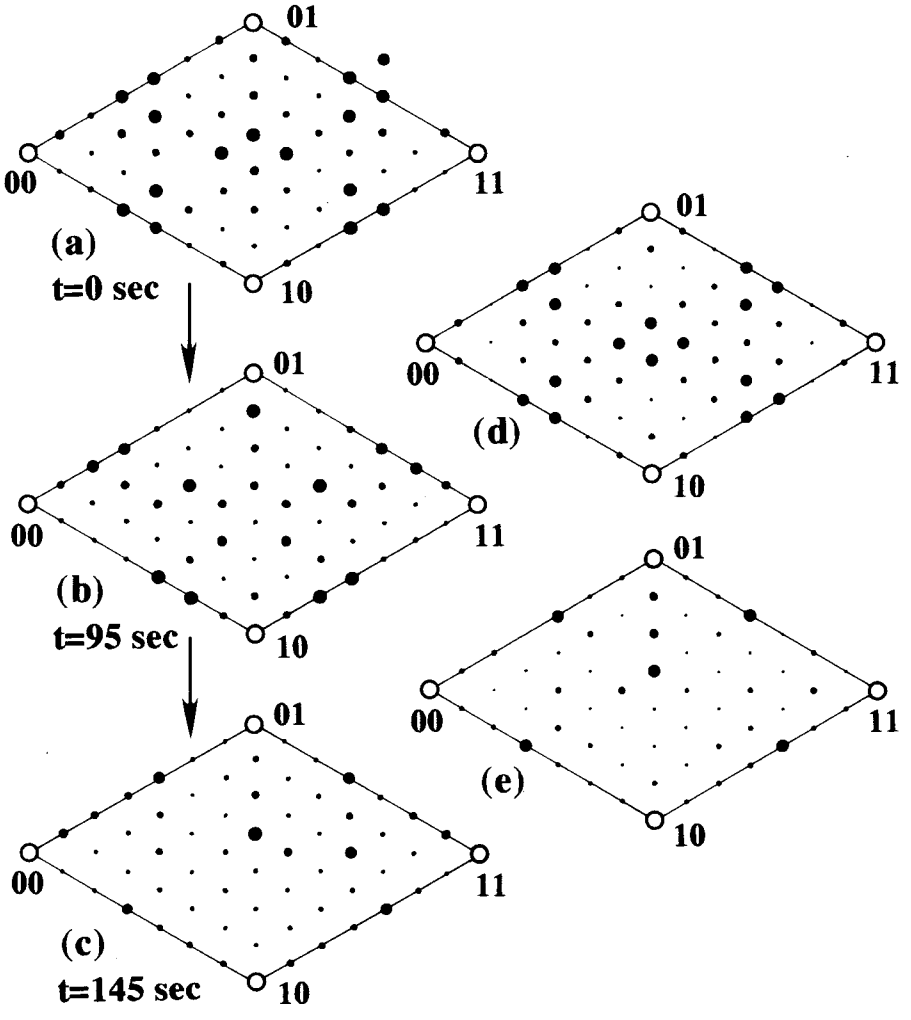


**Figure 10** Two-dimensional reciprocal lattices presenting roughly estimated relative intensities of the 7×7 superlattice spots. (a) is for the clean Si(111)-7×7 surface. (b) and (c) are for the 7×7 surface with room-temperature In adsorption of coverages indicated by "A" and "B" in Fig. 9, respectively. (d) and (e) are kinematically calculated ones for the clean 7×7-DAS surface and for the 7×7 without adatom arrays, respectively.

$\sqrt{7} \times \sqrt{3}$ phase is exactly twice that of the $\sqrt{2} \times \sqrt{2}$, measured from the deposition times for the intensity peaks of the respective spots.

Figure 13 shows the results of simultaneous measurements of the resistance of the Si wafer during In deposition (rate; 0.15 ML/min) onto (a) the clean Si(111)-7 × 7 surface and (b) the Si(111)-$\sqrt{3} \times \sqrt{3}$-In surface at RT (Hasegawa and Ino, 1993). The changes in RHEED patterns are also indicated in the figure. In (a), the resistance does not show significant

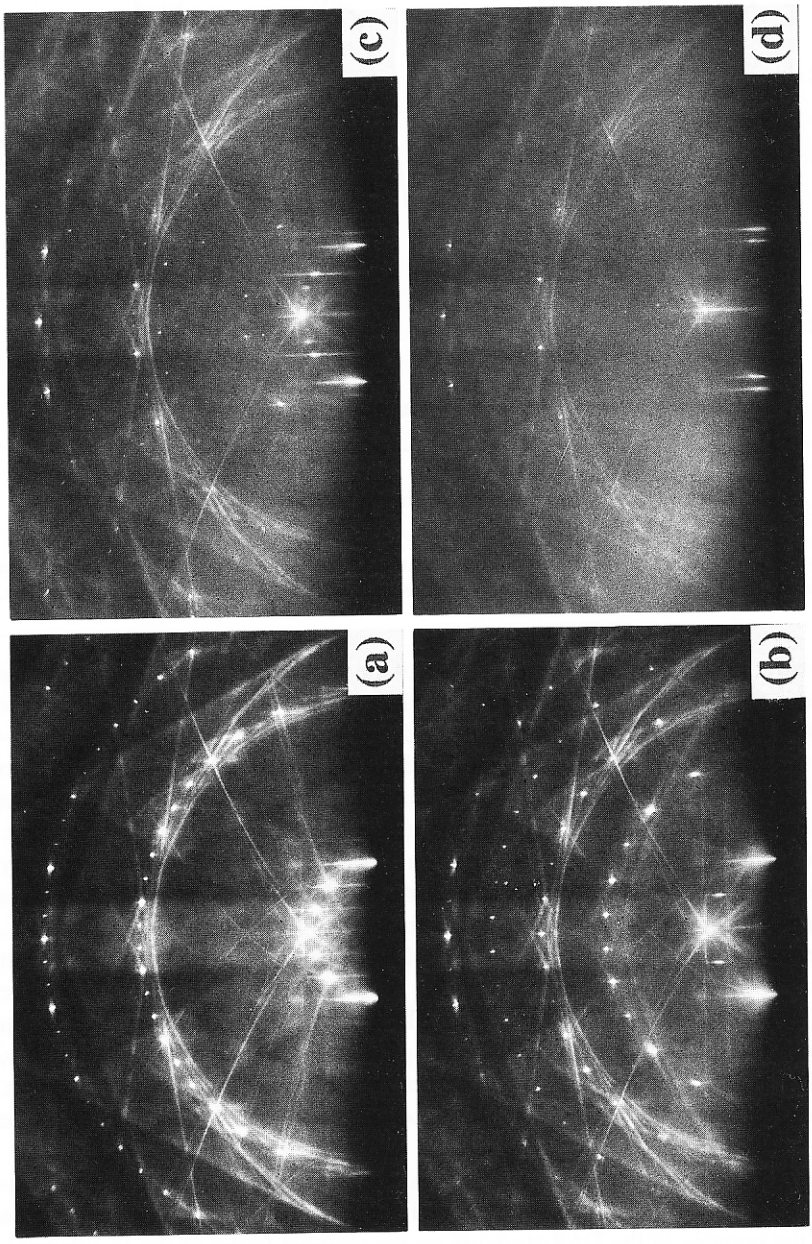


**Figure 11** A series of RHEED patterns during additional In deposition onto the pre-deposited Si(111)-$\sqrt{3}\times\sqrt{3}$-In surface at room temperature; (a) the initial substrate surface, (b) a $2\times2$, (c) a $\sqrt{7}\times\sqrt{3}$, and (d) a $1\times1$+In streaks, reepectively.

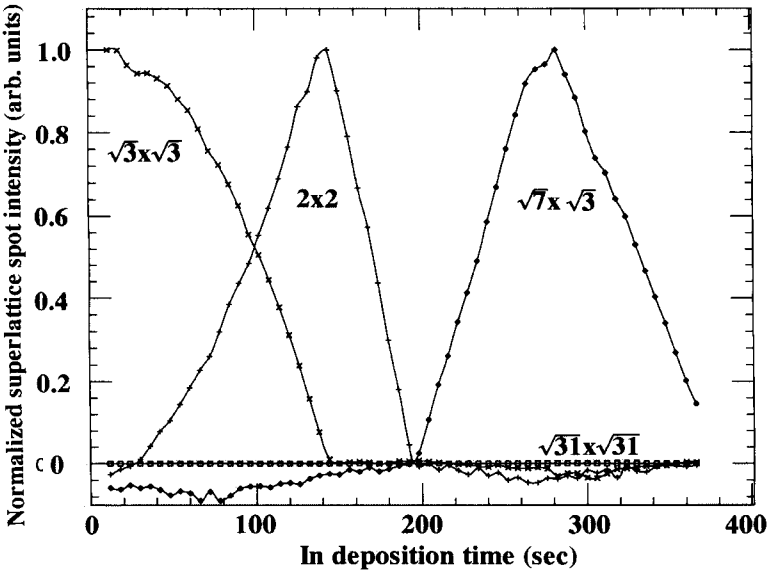


**Figure 12** The changes in the integrated intensities of each superlattice spot appearing during In deposition onto the pre-deposited Si(111)-$\sqrt{3}\times\sqrt{3}$-In surface at room temperature as a function of deposition duration time.

changes up to several ML coverage. Even the onset of the conduction through metal islands is not observed in the thicker coverage range. But this is not so curious because In adatoms have a strong tendency to agglomerate into 3D islands even at RT as revealed by the Debye-Scherrer ring pattern (Baba, Zhou and Kinbara, 1980). In contrast, the In adsorption onto the Si(111)-$\sqrt{3} \times \sqrt{3}$-In surface at RT raises dramatic changes in resistance as shown in (b). With 3 ML coverage the resistance drops down to about one-third of the initial value. This resistance decrease is not monotonic; synchronized with the structure change at every monolayer growth, the resistance drops almost in steps. After this, the resistance remains constant in spite of increase of In coverage. The final value of the resistance with 4 ML coverage depends the deposition rate; with a rate of 0.5 ML/min, the final resistance with 4 ML-In coverage drops to about one-tenth of the initial value. Similar phenomena have been reported by Baba, Zhou and Kinbara (1980). The remarkable and stepwise decrease in resistance is not expected only from the band bending in the Si substrate (Hasegawa and Ino, 1992, 1993). The conduction through the grown metal layer has an important contribution. The conductivity of each phase, $\sqrt{3} \times \sqrt{3}$-In, $2 \times 2$-In, or $\sqrt{7} \times \sqrt{3}$-In, may be quite different.

The difference in adsorption process and epitaxial growth of the In layer on the Si(111)-$7 \times 7$ and Si(111)-$\sqrt{3} \times \sqrt{3}$-In substrates mentioned above may originate from the presence or absence of the remains of the DAS structure on the topmost layers of the Si substrate. It is interesting to recall the experiment of In adsorption on a UHV-cleaved Si(111)-$2 \times 1$ surface at RT (Bolmont, Chen, Sébenne and Proix, 1984). This surface is known to have no stacking fault layer. In this case, the surface structure successively changes in a similar

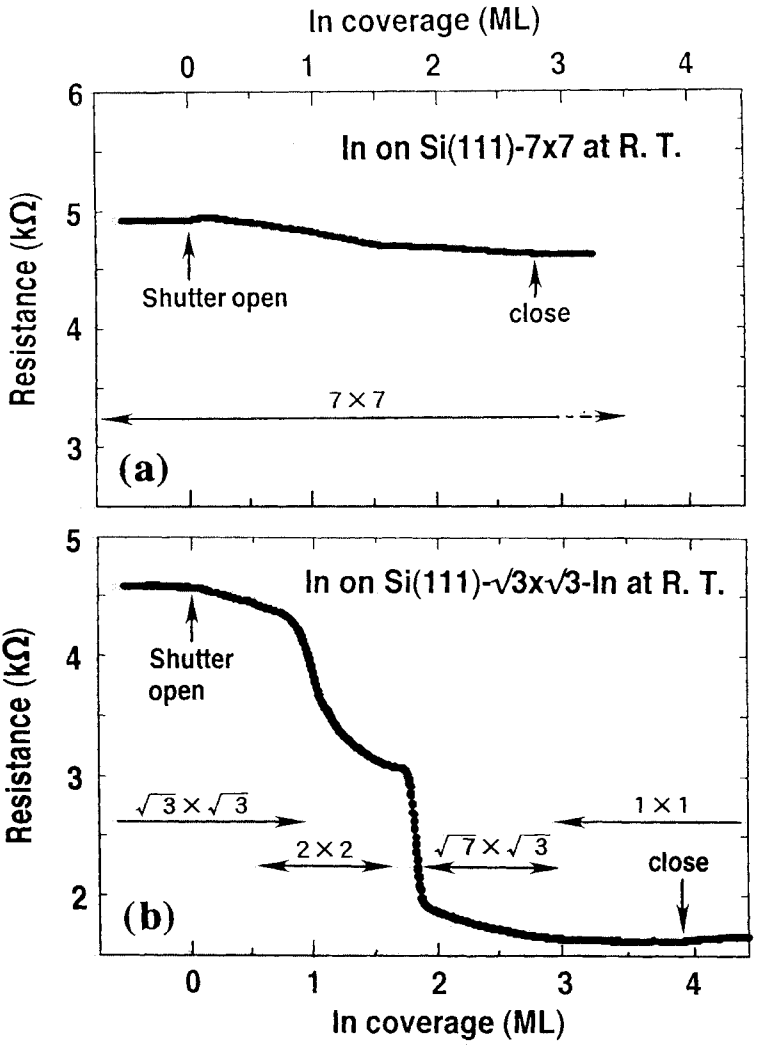


**Figure 13** The changes in resistance of the Si(111) wafer with (a) the 7×7 and (b) the $\sqrt{3}\times\sqrt{3}$-In surface during In deposition (rate = 0.15 ML/min) at room temperature. The RHEED patterns intermittently observed are also indicated in the figure.

way as in the Si(111)-$\sqrt{3} \times \sqrt{3}$-In substrate; from $2 \times 1$ into $\sqrt{3} \times \sqrt{3}$, and then $2 \times 2$. Thus In adatoms are considered to move relatively easily to attain a new ordering on a normal-stacking Si substrate even at RT, whereas the remains of the DAS structure, the dimer-stacking fault framework, on the $7 \times 7$ substrate is not broken by In adsorption, and prevents the surface from converting to a new superlattice at RT.

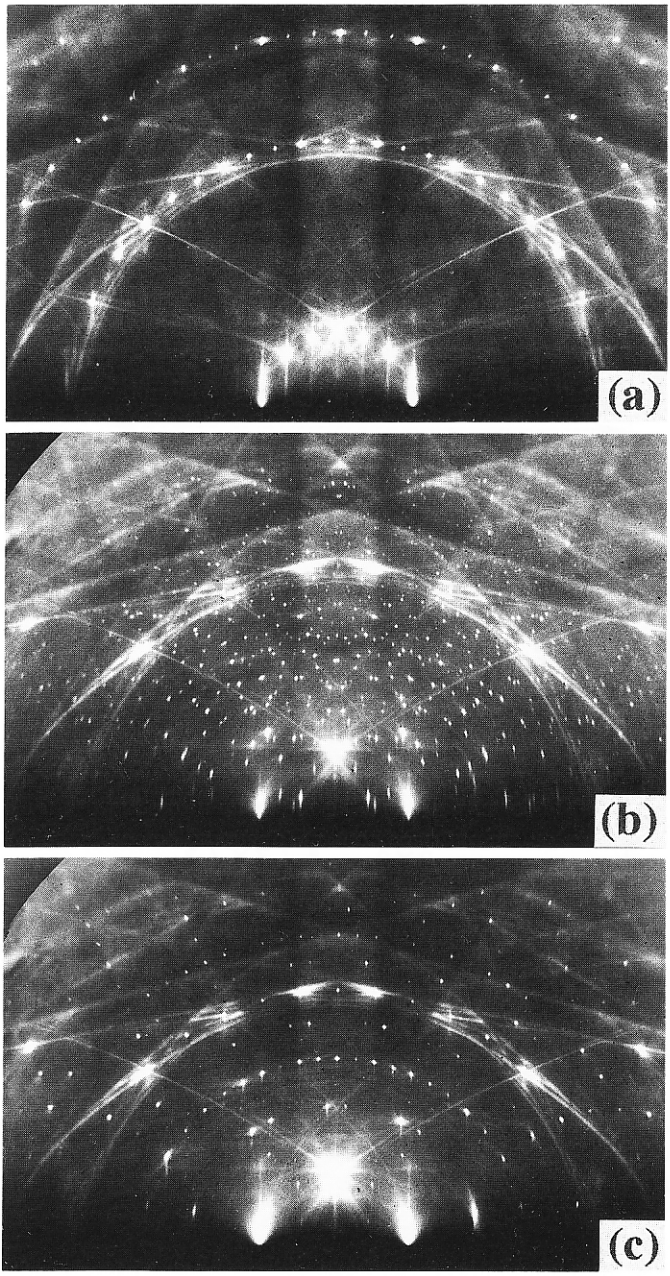


**Figure 14** [11$\bar{2}$]-incidence RHEED patterns taken at room temperature, showing (a) Si(111)-$\sqrt{3}\times\sqrt{3}$, (b) Si(111)-$\sqrt{31}\times\sqrt{31}$-In, and (c) Si(111)-4×1-In phases, respectively, formed with In deposition onto the Si(111) surface at elevated temperatures.

### *3.4 In adsorption on Si(111) at elevated temperatures*

At elevated temperatures completely different restructurings proceed during continuous In deposition. Figure 14 shows the RHEED patterns formed by In depositions onto the elevated-temperature substrate, (a) $\sqrt{3} \times \sqrt{3}$, (b) $\sqrt{31} \times \sqrt{31}$, and (c) $4 \times 1$ superlattices. Sequences of domain conversions among these superstructures sensitively depend on the substrate temperatures. Figure 15 shows the intensity changes of each superlattice spot as a function of nominal In coverage at various substrate temperatures. The abscissa, In coverage, is calibrated such that the maximum intensity of the $\sqrt{3} \times \sqrt{3}$ spot corresponds to $\frac{1}{3}$ ML. This is based on plausible assumption that the sticking probability of In atoms to form the $\sqrt{3} \times \sqrt{3}$ phase is always unity at every temperature. The $7 \times 7$ phase converts to the $4 \times 1$ through a $1 \times 1$ phase at 400°C (a), or $7 \times 7 \rightarrow \sqrt{3} \times \sqrt{3} \rightarrow \sqrt{31} \times \sqrt{31} \rightarrow 4 \times 1$ at 450°C (b), while the $4 \times 1$ structure does not appear at higher temperatures. At 520°C (d), a newly found phase, a $\sqrt{43} \times 4$, appears in a narrow range of coverage between the $\sqrt{3} \times \sqrt{3}$ and the $\sqrt{31} \times \sqrt{31}$ phases. At still higher temperatures, 570°C (e), only the $\sqrt{3} \times \sqrt{3}$ phase is found. By carefully examining the figure, some interesting points are noticed.

(1) A simple expectation is that the maximum intensity of each superlattice corresponds to the saturation coverage for the phase. But the maximum-intensity coverage changes depending on the temperature; for the $4 \times 1$ spot, the intensity peak is at 0.62 ML at 400°C (a), while it is 0.55 ML at 450°C (b). For the $\sqrt{31} \times \sqrt{31}$ spot, the intensity maximum appears at 0.42 ML at 450°C (b), 0.48 ML at 505°C (c), and 0.52 ML at 520°C (d). The temperature dependence of the nominal saturation coverages is caused by changes in the sticking probability of the deposited In atoms and/or changes in the domain sizes of each superstructure.

(2) For the $4 \times 1$ spot in Figs. 15(a) and (b), the spot intensity does not drop to zero, but remains constant, after passing through the intensity maximum, while the spots of the $\sqrt{31} \times \sqrt{31}$ (c) and $\sqrt{3} \times \sqrt{3}$ (e) swiftly disappear to become a $1 \times 1$ with coverage increase. This means the formation of three-dimensional islands on top of the $4 \times 1$ layer, which scarcely cover the surface, while two-dimensional In layers grow on the $\sqrt{31} \times \sqrt{31}$ and $\sqrt{3} \times \sqrt{3}$ phases, destroying the superlattices.

(3) The areal fractions of domains of the respective superstructures, $\sqrt{3} \times \sqrt{3}$, $\sqrt{31} \times \sqrt{31}$, and $4 \times 1$, in (b) seem to change linearly with the increase of In coverage; the sum of the normalized intensities of the two interchanging structures is always almost unity and the intensity curves intersect with each other around the middle. But the transition from the $7 \times 7$ to the $\sqrt{3} \times \sqrt{3}$ phases is not the case; the $\sqrt{3} \times \sqrt{3}$ spot emerges after which the intensity of the $7 \times 7$ spot decreases down to $\frac{1}{5} \sim \frac{1}{10}$ of the initial intensity. This phenomenon is seen also at high temperatures (c)–(e). This means that the $7 \times 7$ domain does not directly convert to the $\sqrt{3} \times \sqrt{3}$ domain; a transient $1 \times 1$ phase is created, and more than a critical amount of the deposited In atoms is necessary for the formation of the $\sqrt{3} \times \sqrt{3}$ domain to be detected by RHEED.

The average size of the $\sqrt{3} \times \sqrt{3}$ domain can be estimated from its spot sharpness (Zuo and Wendelken, 1991). Figures 16(a)(b) show the profiles of the $\sqrt{3} \times \sqrt{3}$-superlattice

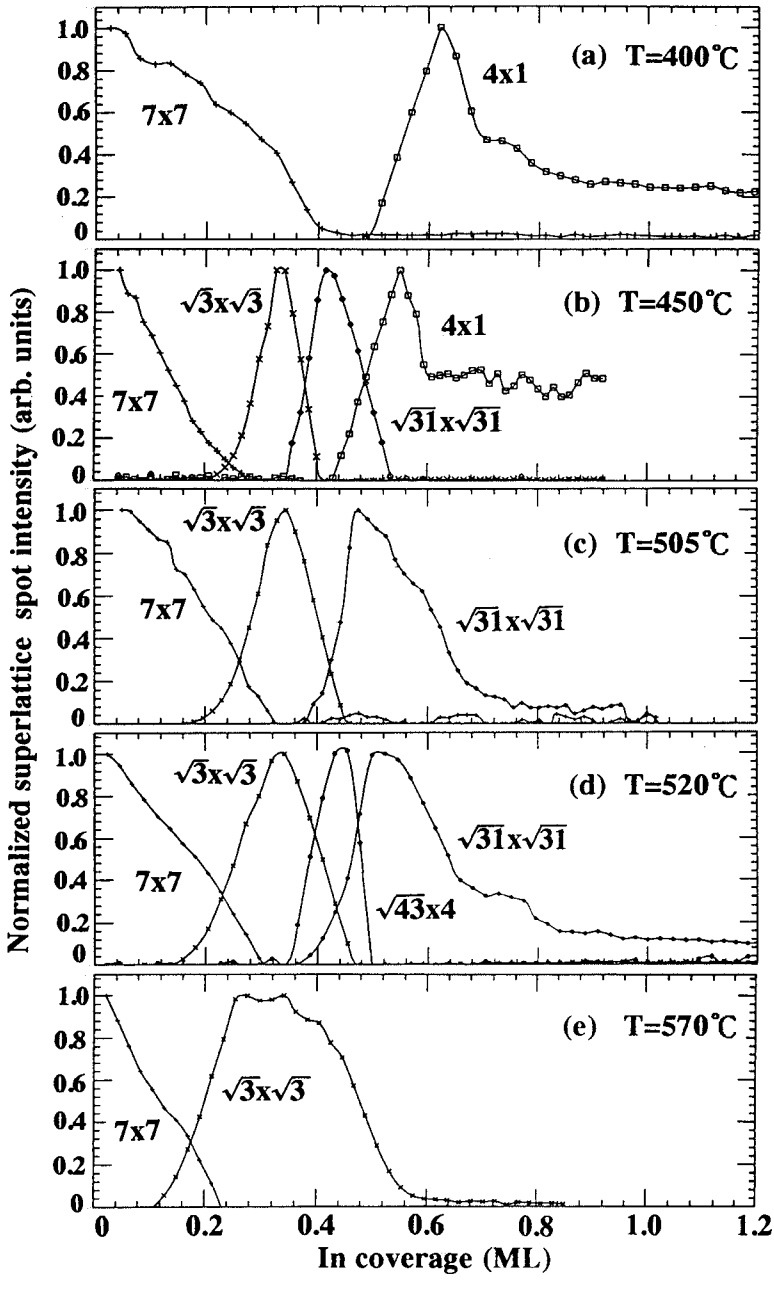


**Figure 15** The growth and decay in the integrated intensity of each superlattice spot appearing during the In deposition onto the clean Si(111)-7×7 surface at elevated temperatures as a function of In coverage.

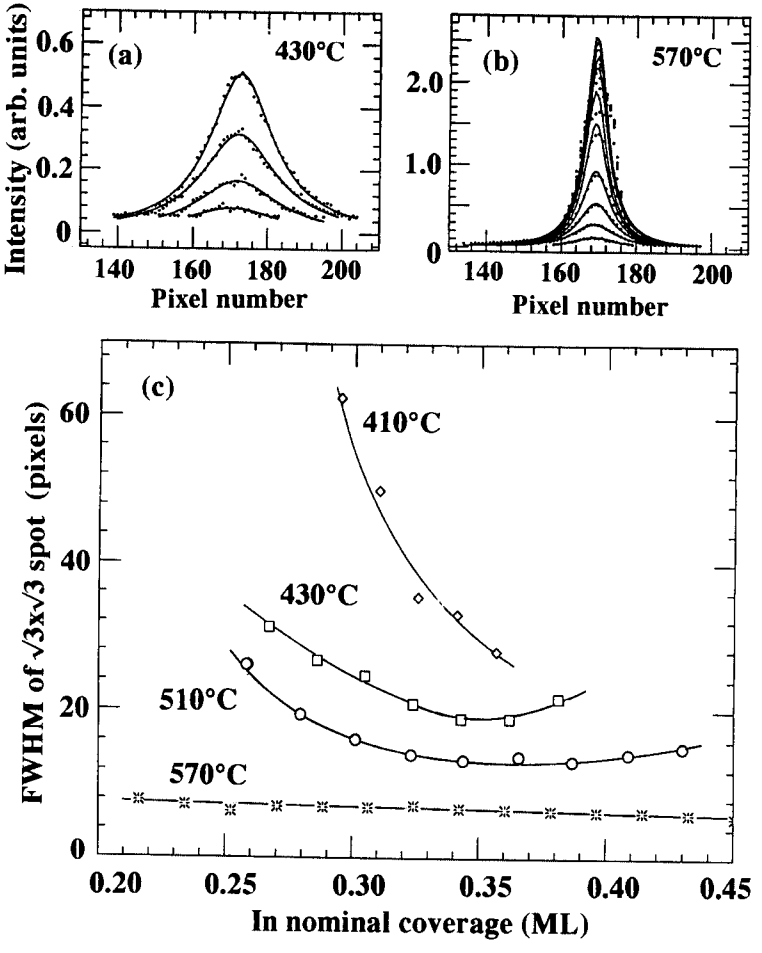


**Figure 16** (a) and (b) are the changes in profiles of the $\sqrt{3}\times\sqrt{3}$ spot along a vertical direction in $[11\bar{2}]$-incidence RHEED pattern during growth by In deposition at 430°C and 570°C, respectively. (c) The In-coverage dependence of the full width at half maximum (FWHM) of the $\sqrt{3}\times\sqrt{3}$ superlattice spots at various substrate temperatures.

spot during its growth with In adsorption at the substrate temperatures of (a) 430°C and (b) 570°C, respectively. The spot in (b) is evidently sharper, meaning larger $\sqrt{3} \times \sqrt{3}$ domains. These spot profiles were fitted with a Lorentzian function and the full widths at half maximum (FWHM) for each spot was deduced. Figure 16(c) shows the changes of the FWHM as a function of In coverage at various substrate temperatures. While the spot width remains a small constant at 570°C, at lower temperatures (410, 430, and 510°C) the broader peaks at smaller coverage range become sharper with coverage increase. This means that the domains of the $\sqrt{3} \times \sqrt{3}$, whose size is larger than the coherence length of the electron beam, is formed from the beginning at 570°C, whereas domain growths of smaller ones

are directly detected at lower temperatures. This is caused by elongation of the diffusion length of deposited In atoms on the surface with temperature increase. The temperature dependence of the diffusion length will more sensitively affect the domain size when more than some critical amount of atoms are necessary for the domain formation, such as in the present $\sqrt{3} \times \sqrt{3}$ case. More quantitative analysis on the growth and decay of the domain is now in progress.

## 4 CONCLUDING REMARKS

As presented here, the integrated intensity of superlattice spots in RHEED provides information on the atomic structure in the unit cell and the areal fraction of the superlattice domain on the surface. The spot profile gives the coherence length of the super lattice periodicity or its averaged domain size. RHEED thus provides the physical nature and various quantities characterizing the dynamic changes of surface structures as well as static structures. Real-space imaging on an atomic-scale resolution will provide complementary information such as seeds of structural conversions and their atomistic mechanism. Studies with both diffraction methods and microscopy are indispensable for fully understanding the phenomena.

*Acknowledgements*

The present study was supported in part by a Grant-In-Aid from the Ministry of Education, Science and Culture of Japan.

*References*

Aiyama, T. and S. Ino (1979). RHEED observation o the Si(111)($\sqrt{31}\times\sqrt{31}$)$R\pm9°$-In structure. *Surf. Sci.*, **82**, L585.

Baba, S., M. Kawaji and A. Kinbara (1979). Isothermal desorption of indium from $\sqrt{31}$-In and $\sqrt{3}$-In on silicon (111) surfaces. *Surf. Sci.*, **85**, 29.

Baba, S., J.M. Zhou and A. Kinbara (1980). Superstructures and growth properties of indium deposits on silicon (111) surface with its influence on surface electrical conduction. *Jpn. J. Appl. Phys.*, **19**, L571.

Baski, A.A., J. Nogami and C.F. Quate (1990). Si(111)-5 × 1-Au reconstrustion as studied by scanning tunneling microscopy. *Phys. Rev.*, **B41**, 10247.

Bauer, E. (1987). Phase Transitions on Single-Crystal Surfaces and in Chemisorbed Layers. In W. Schommers and P. von Blanckenhagen (Eds.), *Structure and Dynamics of Surfaces 2*, Springer, Berlin, pp. 115–180.

Bauer, E. (1991). The Si(111)-(5 × 1) Au structure. *Surf. Sci.*, **250**, L379.

Bennett, P.A. and M.B. Webb (1981). The Si(111)7 × 7 to "1 × 1" transition. *Surf. Sci.*, **104**, 74.

Blandin, A. (1973). Remarks on phase transitions of surfaces. *Phys. Lett.*, **45A**, 275.

Bolmont, D., P. Chen, C.A. Sébenne and F. Proix (1984). Room temperature adsorption and growth of Ga and In on cleaved Si(111). *Surf. Sci.*, **137**, 280.

Chevrier, J., L.T. Vinh and A. Cruz (1992). Phase transition on the Si(111) surfaces: a first order phase transition under strain? *Surf. Sci.*, **268**, L261.

Daimon, H., C. Chungs, S. Ino and Y. Watanabe (1990). A study of Si(111)5 × 2-Au structures by Li adsorption and their coadsorbed superstructures. *Surf. Sci.*, **235**, 142.

Daimon, H. and S. Ino (1985). Study of the Si(111)7 × 7 surface structure by alkali-metal adsorption. *Surf. Sci.*, **164**, 320.

Florio, J.V. and W.D. Robertson (1970). Phase transformations of the Si(111) surface. *Surf. Sci.*, **22**, 459.

Ha, J.S. and E.F. Greene (1989). Observation of phase transitions on the Si(111) and (100) surfaces of Si near 1000K with He atom diffraction. *J. Chem. Phys.*, **91**, 571.

Hansson, G.V., J.M. Nicholls, P. Mårtensson and R.I.G. Uhrberg (1986). Electronic structure of Si(111) surfaces with group III ad-atoms. *Surf. Sci.*, **168**, 105.

Hasegawa, S. and S. Ino (1992). Surface structures and conductance at epitaxial growths of Ag and Au on the Si(111) surface. *Phys. Rev. Lett.*, **68**, 1192.

Hasegawa, S. and S. Ino (1993). Correlation between atomic-scale structures and macroscopic electrical properties of metal-covered Si(111) surfaces. *Int. J. Mod. Phys.*, **B7**, 3817.

Hasegawa, S., Y. Nasal, T. Oonishi and S. Ino (1993). Hysteresis in phase transitions at clean and Au-covered Si(111) surfaces. *Phys. Rev.*, **B47**, 9903.

Horio, Y. and A. Ichimiya (1989). Kinematical analysis of RHEED intensities from the Si(111) 7 × 7 structure. *Surf. Sci.*, **219**, 128.

Horio, Y., A. Ichimiya, S. Kohmoto and H. Nakahara (1991). Kinematical analysis of RHEED patterns from a hydrogen adsorbed Si(111) $\delta 7\times 7$ surface. *Surf. Sci.*, **257**, 167.

Hricovini, K., G. LeLay, M. Abraham and J.E. Bonnet (1990). Phase transitions on the Ge(111) and Si(111) surfaces from core-level studies. *Phys. Rev.*, **B41**, 1258.

Ichikawa, T. and S. Ino (1981). Structural study of Sn-induced superstructures on Ge(111) surfaces by RHEED. *Surf. Sci.*, **105**, 395.

Ino, S. (1977). Some new techniques in reflection high energy electron diffraction (RHEED) application to surface structure studies. *Jpn. J. Appl. Phys.*, **16**, 891.

Ino, S. (1980a). A new structure model for the Si(111)7 × 7 surface structure. *Jpn. J. Appl. Phys.*, **19**, L61.

Ino, S. (1980b). An investigation of the Si(111)7 × 7 surface structure by RHEED. *Jpn. J. Appl. Phys.*, **19**, 1277.

Ino, S.(1988). Experimental overview of surface structure determination by RHEED:. In P.K. Larson and P.J. Dobson (Eds.) *Reflection High-Energy Electron Diffraction and Reflection Imaging of Surfaces*, Plenum, New York, pp. 3–28.

Ishizaka, A., T. Doi and M. Ichikawa (1991). Possibility of a new phase transition in 7 × 7 structure on clean Si(111) surfaces. *Appl. Phys. Lett.*, **58**, 902.

Iwasaki, H., S. Hasegawa, M. Akizuki, S.-T. Li, S. Nakamura and J. Kanamori (1987) Diffuse scattering in the high-temperature (1 × 1) state of Si(111). *J. Phys. Soc. Jpn.*, **56**, 3425.

Izumi, K., T. Takahashi and S. Kikuta (1989). Structural investigation of Si(111) $\sqrt{3}\times\sqrt{3}$-In by low-energy ion-scattering spectroscopy. *Jpn. J. Appl. Phys.*, **28**, 1742.

Kawazu, A. and H. Sakama (1988). Geometric structure of the Si(111) $\sqrt{3}\times\sqrt{3}$-Ga surface. *Phys. Rev.*, **B37**, 2704.

Kitamura, S., T. Sato and M. Iwatsuki (1991). Observation of surface reconstruction on silicon above 800°C using the STM. *Nature*, **351**, 215.

Kohmoto, S. and A. Ichimiya (1989). Determination of the Si(111)"1 × 1" structure at high temperature by reflection high-energy electron diffraction. *Surf. Sci.*, **223**, 400.

Lander, J.J. (1964). Chemisorption and ordered surface structures. *Surf. Sci.*, **1**, 125.

Lander, J.J. and J. Morrison (1964). Surface reactions of silicon with aluminum and with indium. *Surf. Sci.*, **2**, 553.

Latyshev, A.V, A.B. Krasilnikov, A.L. Aseev, L.V. Sokolov and S.I. Stenin (1991). Reflection electron microscopy study of clean Si(111) surface reconstruction during the $(7\times 7)\leftrightarrow(1\times 1)$ phase transition. *Surf. Sci.*, **254**, 90.

McRae, E.G. and R.A. Malic (1985). Low energy electron diffraction beam profiles and phase transition at Si(111)-7 × 7 surface. *Surf. Sci.*, **161**, 5.

Mönch, W. (1993). *Semiconductor Surfaces and Interfaces*, Springer, Berlin, chap. 12.

Murata, Y., M. Kubota and T. Tabata (1992). Phase transition of Si(100) studied by LEED. In A. Yoshimori, T. Shinjo, and H. Watanabe (Eds.) *Ordering at Surfaces and Interfaces*, Springer, Berlin, pp. 93–100.

Nicholls, J.M., P. Mårtensson, G.V. Hansson and J.E. Northrup (1985). Surface states on Si(111) $\sqrt{3}\times\sqrt{3}$-In: Experiment and theory. *Phys. Rev.*, **32**, 1333.

Nielsen, J.A. (1976). Neutron Scattering and Spatial Correlation near the Critical Point. In C. Domb and M.S. Green (Eds.), *Phase transitions and critical phenomena*, Academic, London, pp. 88–165.

Nogami, J., A.A. Baski, and C.F. Quate (1990). $\sqrt{3}\times\sqrt{3}\rightarrow 6\times 6$ phase transition on the Au/Si(111) surface. *Phys. Rev. Lett.*, **65**, 1611.

Nogami, J., S. Park and C.F. Ovate (1987). Indium-induced reconstructions of the Si(111) surface studied by scanning tunneling microscopy. *Phys. Rev.*, **B36**, 6221.

Northrup, J.E. (1984). Si(111) $\sqrt{3}\times\sqrt{3}$-Al: An adatom-induced reconstruction. *Phys. Rev. Lett.*, **53**, 683.

Osakabe, N., Y. Tanishiro, K. Yagi and G. Honjo (1981). Direct observation of the phase transition between the (7 × 7) and (1 × 1) structures of clean (111) silicon surfaces. *Surf. Sci.*, **109**, 353.

Phaneuf, R.J., N.C. Bartelt, E.D. Williams, W. Święch and E. Bauer (1992). LEEM investigations of the domain growth of the (7 × 7) reconstruction on Si(111). *Surf. Sci.*, **268**, 227.

Rivière, J.C. (1990). *Surface Analytical Techniques*, Clarendon, Oxford.

Sakamoto, Y. and J. Kanamori (1993). Lattice gas model of Si(111). *J. Phys. Soc. Japan*, **62**, 563.

Święch, W., E. Bauer and M. Mundschau (1991). A low-energy electron microscopy study of the system Si(111)-Au. *Surf. Sci.*, **253**, 283.

Tabata, T., T. Aruga and Y. Murata (1987). Order-disorder transition on Si(001): c(4 × 2) to (2 × 1). *Surf. Sci.*, **179**, L63.

Takayanagi, K., Y. Tanishiro, M. Takahashi and S. Takahashi (1985a). Structural analysis of Si(111)-7 × 7 by UHV-transmission electron diffraction and microscopy. *J. Vac. Sci. Technol.*, **A3**, 102.

Takayanagi, K., Y. Tanishiro, M. Takahashi and S. Takahashi (1985b). Structure analysis of Si(111)-7 × 7 reconstructed surface by transmission electron diffraction. *Surf. Sci.*, **164**, 367.

Tanishiro, Y., K. Takayanagi and K. Yagi (1983). On the phase transition between the (7 × 7) and (1 × 1) structures of silicon (111) surface studied by reflection electron microscopy. *Ultramicroscopy*, **11**, 95.

Tanishiro, Y., K. Yagi and K. Takayanagi (1990). Gold adsorption processes on Si(111)7 × 7 studied by in-situ reflection electron microscopy. *Surf. Sci.*, **234**, 37.

Telieps, W. and E. Bauer (1985). The (7×7)↔(1×1) phase transition on Si(111). *Surf. Sci.*, **162**, 163.

Tochihara, H., W. Shimada, M. Itoh, H. Tanaka, M. Udagawa and I. Sumita (1992). Structure and restructuring of the atomic steps on Si(111)7 × 7. *Phys. Rev.*, **45**, 11332.

Tsuno, T. (1990). *Adsorption and desorption processes of metal atoms on Si(111) surface investigated by high-energy ion beams*. Ph.D. thesis, University of Tokyo (unpublished).

Yasunaga, H., Y. Kubo and N. Okuyama (1986). Electromigration of In ultrathin film on Si(111). *Jpn. J. Appl. Phys.*, **25**, L400.

Zangwill, A. (1988). *Physics at Surfaces*, Cambridge University Press, p. 113.

Zuo, J.K. and J.F. Wendelken (1991). Substrate temperature effects on $(\sqrt{3}\times\sqrt{3})R30°$ domain growth of Ag on Si(111) surface. *Appl. Surf. Sci.*, **48/49**, 366.